

Research on Spindle and Machining Process Monitoring for Intelligent Machine Tools

Atsushi MATSUBARA¹, Motoyuki SUGIHARA², Ahmed A. D. SARHAN³, Hidenori SARAIE⁴,
Soichi IBARAKI⁵, Yoshiaki KAKINO⁶

¹ Department of Micro Engineering, Graduate School of Engineering, Kyoto University,
Yoshida-honmachi Sakyo-ku Kyoto, Japan 606-8501, matsubara@prec.kyoto-u.ac.jp

² Department of Micro Engineering, Graduate School of Engineering, Kyoto University,
Yoshida-honmachi Sakyo-ku Kyoto, Japan 606-8501, m.sugihara@t01.mbox.media.kyoto-u.ac.jp

³ Department of Precision Engineering, Graduate School of Engineering, Kyoto University,
Yoshida-honmachi Sakyo-ku Kyoto, Japan 606-8501, ah_sarhan@prec.kyoto-u.ac.jp

⁴ Technology R&D, Mori Seiki, 201 Midai Iga-cho Ayama-gun Mie, Japan 519-1414,
saraie@moroseiki.co.jp

⁵ Department of Micro Engineering, Graduate School of Engineering, Kyoto University,
Yoshida-honmachi Sakyo-ku Kyoto, Japan 606-8501, ibaraki@prec.kyoto-u.ac.jp

⁶ Kakino Research Institute, 342-1 Enpukujicho Muromachi-oike-sagaru Nakagyo-ku Kyoto,
Japan 604-8175, kakino@crux.ocn.ne.jp

Summary

This paper describes a monitoring method of the cutting forces for end milling process by using displacement sensors. Four eddy-current displacement sensors are installed on the spindle housing of a machining center so that they can detect the radial motion of the rotating spindle. Thermocouples are also attached to the spindle structure, and the stability of the displacement sensing is examined. The change in spindle stiffness due to the spindle temperature and the speed is investigated as well. Finally, monitoring results of small and medium scale cutting forces in end milling operations are shown as a case study.

Keywords: End milling, Cutting force, Machine tool, Monitoring, Displacement, Spindle

1. Introduction

In order to realize high productive and flexible machining systems, intelligent machining functions have been developed for NC machine tools ⁽¹⁾⁻⁽⁴⁾. Among those intelligent functions for machining centers, monitoring functions of cutting forces are important issues, as they could tell limits of cutting conditions, accuracy of the workpiece, tool wear, and other process information, which are indispensable for process feedback control. In the researches on cutting force monitoring, there are two approaches: internal sensor approach and external sensor approach. Some researchers have succeeded in the cutting force monitoring by utilizing motor currents in CNC-Servo systems ⁽⁵⁾⁽⁶⁾. However, it is difficult to use motor currents for the monitoring of cutting forces in an end-milling process, since the magnitude and the direction of cutting forces change frequently and the friction change on guideways influences the monitoring accuracy. For such applications, external sensor approach is promising, and there are many researches on cutting force monitoring by using several types of sensors such as strain gauges, force sensors, acceleration sensors and so on ⁽⁷⁾⁽⁸⁾.

Among those external sensors, the authors have employed displacement sensors ⁽⁹⁾, as they are cheap and small enough to be built in the spindle structure. Displacement signals are translated into cutting force information by the calibration. However, the monitoring quality in the long term is a problem, because sensors also detect the displacement caused by thermal effects. In this research, we develop a spindle with displacement sensors and thermal sensors to monitor the spindle displacement and stiffness. First, we investigate the behavior of the spindle displacement in radial direction by using four displacement sensors. Second, the change in spindle stiffness due to the spindle speed and temperature is investigated. Finally, tests for the monitoring of cutting forces in end milling operations are carried out.

2. Measurement of the spindle displacement

2.1 Experimental set-up

In order to develop monitoring functions, displacement sensors and thermal sensors are installed on the spindle unit of a high precision machining center. The machine used in the study is a vertical-type machining center (GV503 made by Mori Seiki). The spindle has constant position preloaded bearings with oil-air lubrication, and the maximum rotational speed is 20000 rpm. Four eddy-current displacement sensors are installed on the housing in front of the bearings to detect the radial motion of the rotating spindle. The specifications of the sensor are as follows: measurement range is 1mm; nominal sensitivity is 0.2 mm/V; dynamic range is 1.3 kHz; linearity is $\pm 1\%$ of full scale. Figure 1 shows the sensor locations. The two

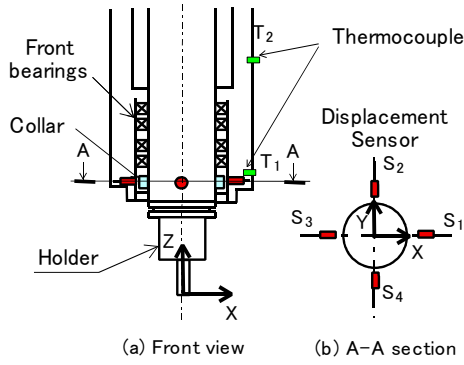


Fig.1 Locations of the sensors

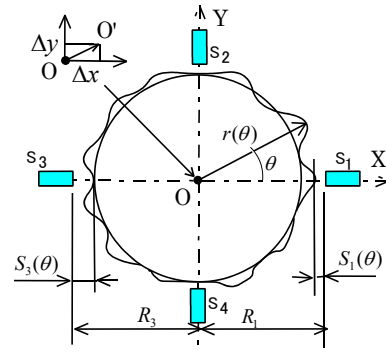


Fig.2 The concept of the displacement measurement

sensors, S_1 and S_3 , are aligned opposite in X direction, and the other two, S_2 and S_4 , are aligned opposite in Y direction. In order to measure spindle temperature, several thermocouples are attached to the spindle structure. Those thermocouples include T_1 and T_2 shown in Fig.1. T_1 is installed on the bearing retaining cover, and T_2 is installed on the body of the spindle unit, which is near the windings of the built-in motor.

2.2 The concept of the displacement measurement

Figure 2 shows the concept of the spindle displacement measurement. When the spindle axis shifts by Δx μm in X direction due to the cutting force and thermal effects, the displacement signals from S_1 and S_3 are as follows.

$$S_1(\theta) = G[R_1 - r(\theta) - \Delta x] \quad (1)$$

$$S_3(\theta) = G[R_3 - r(\theta + \pi) + \Delta x] \quad (2)$$

where G : sensor sensitivity [$\text{mV}/\mu\text{m}$], R_i : the distance between the spindle center and detection surface of the sensor S_i [μm] ($i=1, \dots, 4$), θ : rotation angle of the spindle [rad], $r(\theta)$: the sum of the radial error motion and surface roughness of the sensor target [μm].

Subtracting the displacement signals and dividing the subtraction by two, we obtain

$$S_x(\theta) = [S_3(\theta) - S_1(\theta)] / 2 \quad (3)$$

Letting $S_x(\theta) = S_{x0}(\theta)$ such that $\Delta x = 0$, and subtracting $S_{x0}(\theta)$ from $S_x(\theta)$

$$S_x(\theta) - S_{x0}(\theta) = G \cdot \Delta x \quad (4)$$

then we obtain the axis shift Δx as follows.

$$\Delta x = [S_x(\theta) - S_{x0}(\theta)] / G \quad (5)$$

Similarly, the axis shift in Y direction, Δy , is calculated from the displacement signals from S_2 and S_4 . The axis shift is called the spindle displacement hereafter.

2.3 Experimental result

For the measurement of the spindle displacement due to the cutting forces, the sensor signals should be stable for any other disturbance. To check the stability of the sensing, the spindle displacement and temperature are measured during the spindle rotation without cutting. The spindle is started at 3000 rpm and kept rotating for 1 hour. After that the spindle speed is increased to 6000 and 9000 rpm for every hour. Figure 3 shows an example of measured displacement signals at the spindle speed of 6000 rpm. Figure 4 shows the subtraction signals of the opposite sensors. As shown in Fig. 3, all the sensor signals involve two types of fluctuation: a transient response type and a periodic type. These fluctuations appear in the spindle displacement, and they are remaining in the subtraction signals shown in Fig. 4. Figure 5 shows the measured spindle temperature. The transient response can be seen in the temperature measured by the sensor T_1 , and the

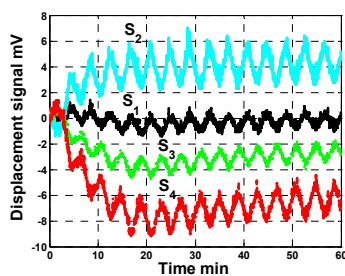


Fig.3 Displacement signals (Spindle speed: 6000rpm)

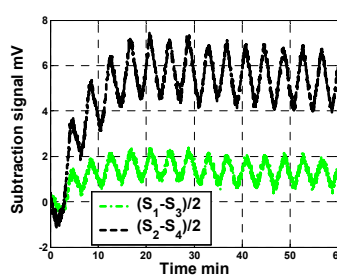


Fig.4 Subtraction signals

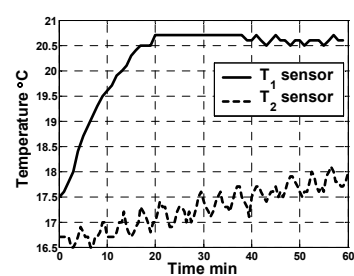


Fig.5 Spindle temperature

periodic fluctuation can be seen in the sensor T_2 . The same fluctuations are also observed in the measurement results at other spindle speeds, but the periodicity and range are different for each spindle speed. The transient fluctuation type is related to thermal extension of the spindle, while the periodic fluctuation type is related to the cooling control of the oil, which is circulating inside the spindle body.

3. Measurement of the spindle stiffness

3.1 Experimental procedure

In the previous section, it can be seen that the fluctuation of the spindle displacement depends on the spindle temperature. Therefore, we can compensate the fluctuation by monitoring the spindle temperature. For the monitoring of cutting forces, however, the spindle stiffness should be constant in the cutting process. For this reason, characterization of the spindle stiffness in radial direction should be investigated as well as the factors that affect the spindle stiffness. It is well known that the spindle speed and the temperature change the state of ball contact and the preload of the bearing systems. Therefore, it is likely that the spindle speed and temperature influence the spindle stiffness. For this reason we investigate the effect of these parameters on the spindle stiffness.

For the measurement of the spindle stiffness in the radial direction, the load in this direction is necessary to deflect the spindle and to be measured precisely. The static loading test is widely used to evaluate the overall stiffness of machine tools. The stiffness obtained by the static test, however, typically shows hysteresis characteristics, because the contact area of the bearing changes as the load direction changes. More importantly, the static stiffness is different from the stiffness of the rotating spindle. Therefore we carry out the cutting test to provide dynamic load and measure the cutting forces with a table type tool dynamometer (Model 9257B made by Kistler). Figure 6 shows the tool path for the cutting test. The tool moves along the X-axis with variable radial depth of cut from 0 to 1 mm. In the -X direction the cutting mode is down-cut, while in the +X direction it is up-cut. To remove residual stock, each path is repeated. The cutting time for one operation is about 4 s, which is short enough to avoid the thermal disturbances. Table 1 shows the cutting conditions. After the spindle is rotated at 3000 rpm without cutting for 20 min (the 1st warm up), the 1st cutting test is carried out at three spindle speeds. Then the spindle is warmed up again at the speed of 6000 rpm for 30 min without cutting. The same cutting test (the 2nd cut) is repeated, and followed by the spindle warm-up operation at the speed of 9000 rpm for 30 min. Finally the 3rd cut is carried out.

The spindle displacement signals are digitized with a 16-bit A/D board, and the cutting force signals (X, Y, and Z direction) from the dynamometer are digitized with a 12-bit A/D board. For the measurement of rotational angle of the spindle, A, B, and Z pulses of the rotary encoder, which is originally used for the spindle speed control, are counted with a 32bit-counter board. The sampling frequency is set so that 40 points per one spindle revolution can be obtained. The subtraction of the digitized signals of the opposite sensors in one rotation, $S_{j0}(m)$ ($m=1,\dots,40$, $j=x, y$), are recorded in the PC memory prior to the cutting. When the cutting is started and the subtraction signal points for one revolution, $S_j(m)$, are obtained, then $S_{j0}(m)$ are subtracted for each index m . The subtraction data are filtered by a moving average filter. Thus the spindle displacements in X and Y directions are obtained and compared with measured cutting forces.

3.2 Experimental results

After the 1st warm-up term, the spindle temperature is around 19 °C. The increase of the spindle temperature is 2 °C in the 2nd and 3rd warm-up term, respectively. Figure 7 shows an example of the relationships between the spindle displacement and cutting force. As shown in Fig.7, the relation can be approximated linearly, but the y-section of the line is not zero because of the nonlinearity around the origin. As other relationships obtained in the different conditions show the same tendency, the spindle stiffness is identified by using linear approximation.

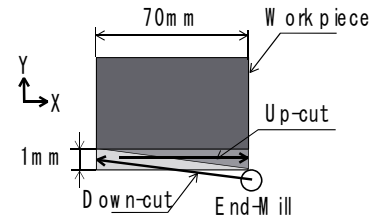


Fig. 6 Workpiece and tool paths

Table 1 Cutting conditions

Spindle speed (rpm)	3000, 6000, 9000
Feed per tooth (mm/tooth)	0.167
Axial depth of cut (mm)	10
Cutting tool	Coated carbide end mill, diameter: 10 mm, numbers of flute: 4
Coolant	Air
Workpiece material	Carbon steel

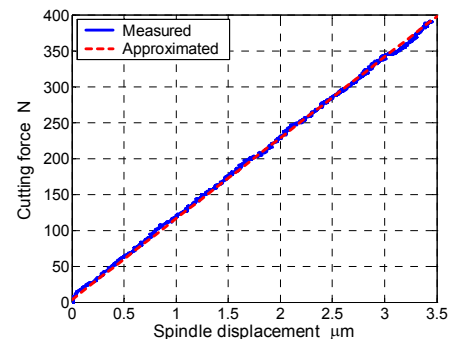


Fig.7 An example of the relationship between the spindle displacement and the cutting force (direction: X-axis, spindle speed: 3000rpm, cutting mode: up-cut, spindle temperature: 19.8 °C)

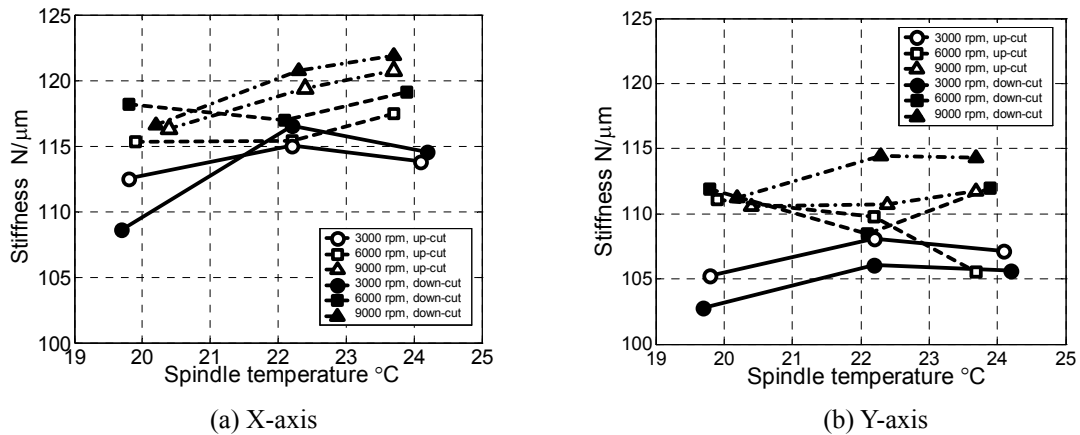


Fig.8 Identified spindle stiffness on different cutting conditions

Figure 8 shows the identified spindle stiffness on different cutting conditions. The spindle stiffness indicates slight correlation with the spindle temperature and speed. As for the stiffness data at the spindle speed of 3000 rpm in down cut, the estimated stiffness is smaller than that of other conditions. Checking the force range of the data, we found that the air-cut term is not long enough to get the same force range as other ones. This indicates the existence of nonlinearity in force-displacement relationship, but we assume that the spindle stiffness is constant and average the stiffness data that has force range of 0-400N. The estimated spindle stiffness is $117 \text{ N}/\mu\text{m}$ in X direction, and $110 \text{ N}/\mu\text{m}$ in Y direction. The reason of slight difference in the stiffness between X and Y-axis might come from the sensitivity difference of each sensor, as we use the nominal sensitivity value for each sensor.

4. Case study on monitoring of cutting forces

In this Section, a cutting test is carried out to validate the monitoring performance. A cutting process of a rectangular pocket feature is selected as a case study, as several sub-processes are involved in the entire cutting process. The entire process consists of the following sub-processes: (a) boring with helical cycles, (b) circle enlargement with spiral cycles, (c) slotting with trochoidal cycles, and (d) corner rounding with trochoidal cycles. Figure 9 shows the workpiece and the tool paths used in each process. We use the same cutting tool as shown in Table 1. The spindle speed is 3000 rpm, and the axial depth of cut is 10mm. As each process has different feed rates and radial depths of cut, the entire process monitoring is a difficult subject. Spindle displacements in X and Y-axis are monitored by using the same measurement system shown in Section 3.1. Cutting forces are estimated by multiplying measured spindle displacements and the stiffness identified in Section 3.2. The results are compared with cutting forces measured with the dynamometer. The spindle temperature T1 and T2 are monitored simultaneously.

By comparing the estimated and measured cutting forces in each process, monitoring errors (measured minus estimated) are calculated. Figure 10 shows the comparison of the estimated and measured cutting force in the helical boring process; Figure 11 shows the monitoring errors. In the helical boring process, the components of the monitoring error are a periodic error and a drift error. The spindle temperature T1 has the small range of fluctuation in the entire term, but the spindle temperature T2 has the periodic fluctuation. The periodic temperature fluctuation corresponds to the drift error in Fig.11.

Figure 12 and 13 shows results in the trochoidal slotting process. Figure 14 shows the estimated and measured cutting forces in the one cycle. As can be seen in Fig. 14, the time lag is observed between the estimated and measured profiles. Moreover, the measured profile does not reach estimated one at the bottom. So the spindle stiffness seems to be a little larger than the true value when the cutting force is over 400 N. As the experimental data set that is used for the identification of the spindle stiffness ranges from 0 to 400N, the spindle stiffness are to be re-modeled for the monitoring

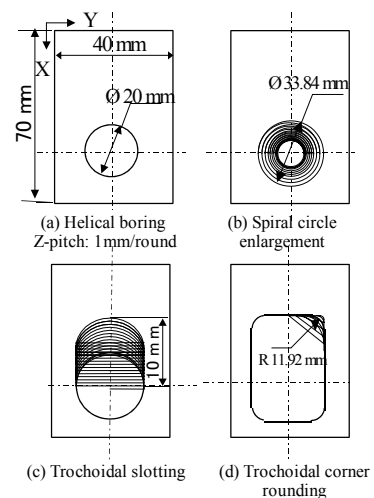


Fig.9 Workpiece and tool paths used in each process

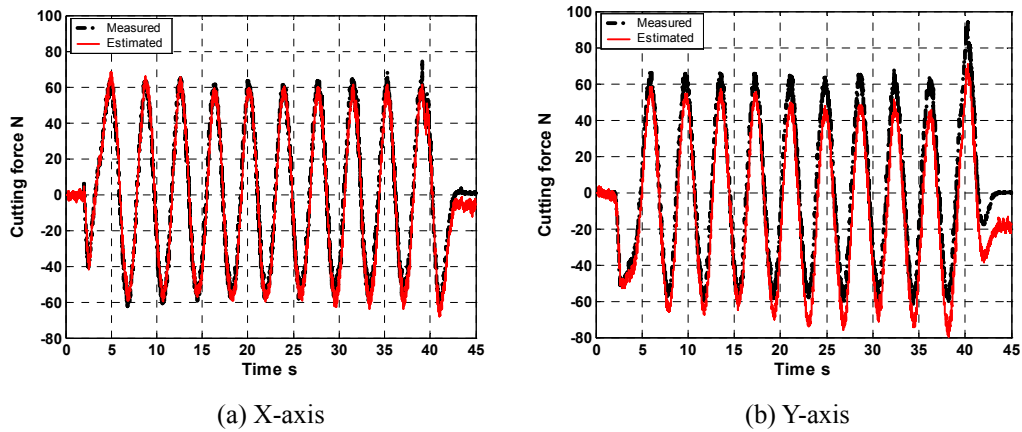


Fig.10 Comparison of the estimated and measured cutting force in helical-cut

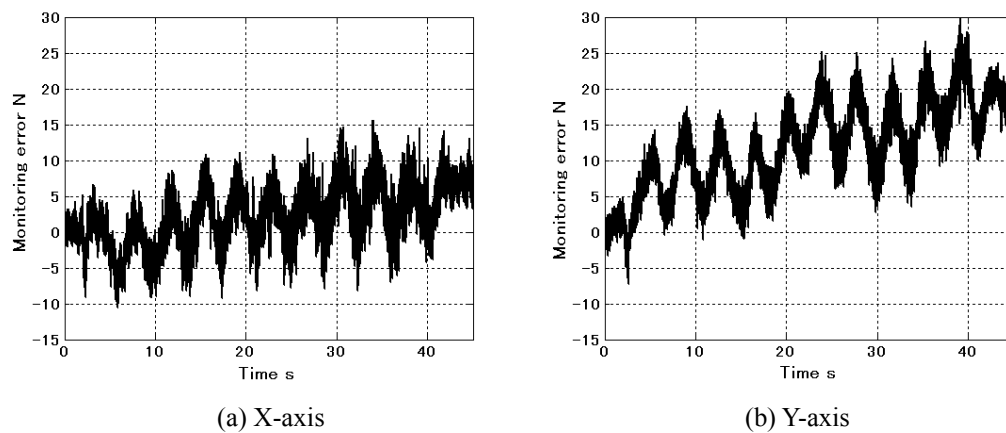


Fig.11 Monitoring error (measured minus estimated cutting force) in helical-cut

of lager cutting forces.

The monitoring errors in each process are summarized in Table 2. The large estimation errors in the spiral cut are caused by the same reason as shown in the trochoidal-cut: time lag and modeling error of the spindle stiffness.

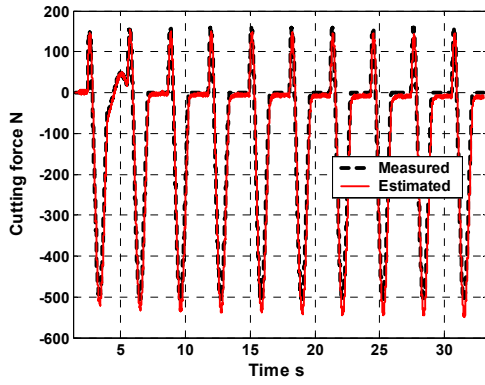
5. Conclusion

Displacement sensors and thermocouples are installed on the spindle structure of a machining center for the monitoring of cutting forces. From the several experiments, following results are obtained:

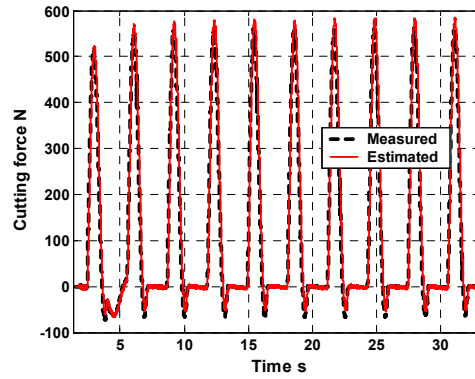
- (1) The drifts in the displacement signals are caused by the thermal deformation of the spindle.
- (2) The temperature increase due to the spindle rotation has a little effect on the change of the spindle stiffness.
- (3) The causes of monitoring error are the thermal displacement of the spindle, the time lag of the sensing system, and the modeling error of the spindle stiffness.

References

- (1) M. Mitsuishi, S. Warisawa and R. Hanayama, Development of an Intelligent High-Speed Machining Center, Annals of the CIRP, 50-1(2001), p.275-280.
- (2) K. Yamazaki, Y. Hanai, M. Mori and K. Tezuka, Autonomously Proficient CNC Controller for High-Performance Machine Tools Based on an Open Architecture Concept, Annals of the CIRP, 46-1(1997) , p.275-278
- (3) M. Mori, K. Yamazaki, M. Fujishima, J. Liu and N. Furukawa, A Study on Development of an Open Servo System for Intelligent Control of a CNC Machine Tool, Annals of the CIRP, 50-1(1997), p.247-250
- (4) M. Kaever, N. Brouer, M. Rehse and M. Weck, NC Integrated Process Monitoring and Control for Intelligent Autonomous Manufacturing Systems, 29th CIRP International Seminar on Manufacturing Systems, Osaka(1997), p.69-74.
- (5) Y. Altintas : Prediction of Cutting Forces and Tool Breakage in Milling form Feed Drive Current Measurements, ASME Journal of Engineering for Industry, Vol.114, (1992), p.386-392.

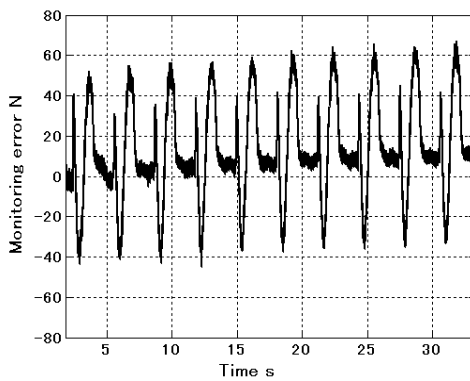


(a) X-axis

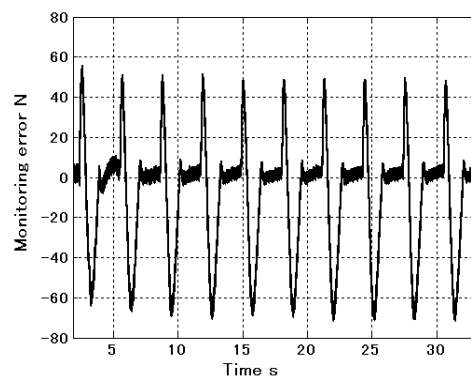


(b) Y-axis

Fig.12 Comparison of the estimated and measured cutting force in trochoidal-cut



(a) X-axis



(b) Y-axis

Fig.13 Monitoring error (measured minus estimated cutting force) in trochoidal-cut

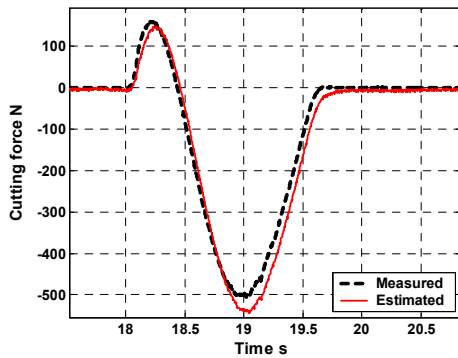


Fig. 14 Cutting forces in one cycle (enlargement of Fig.12(a))

Table 2 Monitoring errors in each process

Process	Axis	Monitoring errors N	
		Upper	Lower
Helical-cut	X	15.6	- 10.6
	Y	29.8	- 7.3
Spiral-cut	X	94.9	- 81.7
	Y	91.6	- 117.2
Trochoidal-cut	X	67.3	- 45.2
	Y	55.9	- 72.0
Corner-cut	X	24.4	- 43.9
	Y	24.9	- 53.2

- (6) H. Saraie, M. Sakahira, S. Ibaraki, A. Matsubara, Y. Kakino, M. Fujishima, Monitoring and Adaptive Control of Cutting Force Based on Spindle Motor Currents in Machining Centers, Proc. of the 2nd International Conference of LEM21, Nigata, Japan, Nov.(2003), p555-560.
- (7) G. Byrne, D. Dornfeld, I. Inasaki, G. Ketteler, W. Konig and R. Teti, Tool Condition Monitoring (TCM)—Status of Research and Industrial Application—, Annals of the CIRP, 44-2(1995), p.541-567.
- (8) J. F. Tu, M. Corless and J. Jeppson, Robust Control of High Speed End Milling with Unknown Process Parameter and CNC Delay, Proceedings of 2002 Japan-USA Symposium of Flexible Automation, Hirohima, July 14-19 (2002).
- (9) A. D. Sarhan, A. Matsubara, S. Ibaraki, Y. Kakino, Monitoring of Cutting Force using Spindle Displacement Sensor, Proc. of the 2004 Japan-USA Symposium on Flexible Automation, Denver, July 19-21(2004), JS023.